

Characterization of a Structural Leoligin Analog as Farnesoid X Receptor Agonist and Modulator of Cholesterol Transport[#]

Authors

Angela Ladurner¹, Thomas Linder², Limei Wang¹, Verena Hiebl¹, Daniela Schuster^{3,4}, Michael Schnürch², Marko D. Mihovilovic², Atanas G. Atanasov^{1,5,6,7}, Verena M. Dirsch¹

Affiliations

- 1 Department of Pharmacognosy, Faculty of Life Sciences, University of Vienna, Vienna, Austria
- 2 Institute of Applied Synthetic Chemistry, TU Wien, Vienna, Austria
- 3 Department of Pharmacy/Pharmaceutical Chemistry and Center for Molecular Biosciences Innsbruck (CMBI), University of Innsbruck, Innsbruck, Austria
- 4 Department of Pharmaceutical and Medicinal Chemistry, Institute of Pharmacy, Paracelsus Medical University, Salzburg, Austria
- 5 Institute of Genetics and Animal Breeding of the Polish Academy of Sciences, Jastrzebiec, Poland
- 6 Institute of Neurobiology, Bulgarian Academy of Sciences, Sofia, Bulgaria
- 7 Ludwig Boltzmann Institute for Digital Health and Patient Safety, Medical University of Vienna, Vienna, Austria

Key words

farnesoid X receptor, leoligin, structural analog, lignan, cholesterol efflux, cholesterol uptake

received January 14, 2020

revised April 24, 2020

accepted May 5, 2020

Bibliography

DOI <https://doi.org/10.1055/a-1171-8357>

published online | Planta Med © Georg Thieme Verlag KG
Stuttgart · New York | ISSN 0032-0943

Correspondence

Dr. Angela Ladurner

Department of Pharmacognosy, Faculty of Life Sciences,
University of Vienna

Althanstraße 14, A-1090 Vienna, Austria

Phone: + 43 1 427 75 52 39, Fax: + 43 1 427 75 59 69

angela.ladurner@univie.ac.at



Supporting information available online at
<http://www.thieme-connect.de/products>

ABSTRACT

The ligand-activated farnesoid X receptor is an emerging therapeutic target for the development of drugs against metabolic syndrome-related diseases. In this context, selective bile acid receptor modulators represent a novel concept for drug development. Selective bile acid receptor modulators act in a target gene- or tissue-specific way and are therefore considered less likely to elicit unwanted side effects. Based on leoligin, a lignan-type secondary plant metabolite from the alpine plant *Leontopodium nivale* ssp. *alpinum*, 168 synthesized structural analogs were screened in a farnesoid X receptor *in silico* pharmacophore-model. Fifty-six virtual hits were generated. These hits were tested in a cell-based farnesoid X receptor transactivation assay and yielded 7 farnesoid X receptor-activating compounds. The most active one being LT-141A, with an EC₅₀ of 6 μM and an E_{max} of 4.1-fold. This analog did not activate the G protein-coupled bile acid receptor, TGR5, and the metabolic nuclear receptors retinoid X receptor α, liver X receptors α/β, and peroxisome proliferator-activated receptors β/γ. Investigation of different farnesoid X receptor target genes characterized LT-141A as selective bile acid receptor modulators. Functional studies revealed that LT-141A increased cholesterol efflux from THP-1-derived macrophages via enhanced ATP-binding cassette transporter 1 expression. Moreover, cholesterol uptake in differentiated Caco-2 cells was significantly decreased upon LT-141A treatment. In conclusion, the leoligin analog LT-141A selectively activates the nuclear receptor farnesoid X receptor and has an influence on cholesterol transport in 2 model systems.

[#] Dedicated to Professor Dr. Wolfgang Kubelka on the occasion of his 85th birthday.

ABBREVIATIONS

| | |
|-------|--|
| ABCA1 | ATP-binding cassette transporter 1 |
| BSEP | bile salt export pump |
| CDCA | chenodeoxycholic acid |
| CETP | cholesteryl ester transfer protein |
| FXR | farnesoid X receptor |
| HMGCR | 3-hydroxy-3-methyl-glutaryl-CoA reductase |
| LXR | liver X receptor |
| PBC | primary biliary cholangitis |
| PMA | phorbol 12-myristate 13-acetate |
| PPAR | peroxisome-proliferator-activated receptor |
| RXR | retinoid X receptor |
| SBARM | selective bile acid receptor modulator |
| SHP | small heterodimer partner |

Introduction

In the last decades, metabolic syndrome-related diseases have become an increasing public health issue [1]. Many metabolic pathways are regulated by nuclear receptors. These receptors act as ligand-activated transcription factors, thereby regulating the expression of target genes involved in processes like lipid, glucose, and cholesterol metabolism. One of these nuclear receptors is the farnesoid X receptor (FXR). Endogenously, FXR is activated by bile acids, which are synthesized from cholesterol in the liver [2, 3]. FXR-dependent gene regulation results in downregulation of lipogenesis in the liver as well as bile acid synthesis from cholesterol, hepatic bile acid uptake, and intestinal absorption. Bile acid modification and secretion, on the other hand, are upregulated by FXR [4]. Altogether, this depicts the importance of FXR in metabolic processes, and cholesterol metabolism in particular. FXR is mainly expressed in metabolic tissues such as the liver and intestine but also in the kidney and adrenal glands and to a lesser amount in macrophages [5, 6]. The therapeutic potential of FXR lies in the treatment of cholestatic liver diseases, hypercholesterolemia, hypertriglyceridemia, nonalcoholic steatohepatitis, and type 2 diabetes mellitus [7]. Of note, 1 FXR agonist, obeticholic acid (Ocaliva), has already been approved in the U.S. and Europe in a fast track procedure for the treatment of primary biliary cholangitis (PBC) [8]. Despite its beneficial impact in the therapy of PBC, obeticholic acid has several adverse effects, such as pruritus, fatigue, and gastrointestinal symptoms. Moreover, disadvantageous serum lipid and cholesterol profiles may occur with FXR agonist treatment [9, 10]. Thus, it is of great interest to develop novel FXR modulators with a minimal side effect profile and with a wide area of treatment indications.

High affinity full agonists of FXR activate the whole plethora of FXR target genes and are therefore more likely to elicit undesirable effects. Therefore, increasing focus is directed at the identification and development of selective bile acid receptor modulators (SBARM) that act in a tissue- or gene-specific manner with the ultimate goal to design FXR agonists for specific therapeutic purposes (reviewed in [8]). This aim is very challenging as the mechanisms underlying gene- and tissue-selectivity are still being elucidated. Several hypotheses about how to achieve selectivity have

been proposed, including differential cofactor or DNA binding, transactivation *versus* transrepression, and binding of ligands to allosteric pockets (S2 pocket) [8].

In the basal state, FXR resides in the nucleus and is bound together with its heterodimer partner, the retinoid X receptor (RXR), to respective response elements in promoter regions of target genes together with co-repressors. Upon the binding of full agonists, like obeticholic acid and the endogenous agonist chenodeoxycholic acid (CDCA), conformational changes lead to the release of these co-repressors and to the binding of co-activators, resulting in target gene expression. In contrast to full FXR agonists, SBARMs are partial agonists. The molecular basis of differential modes of FXR modulation has been investigated recently and shows that the partial agonists DM175 and ivermectin can recruit co-activator and co-repressor peptides at the same time, thereby eliciting a fluid FXR modulation profile [11].

FXR can be activated by different compounds from diverse sources, including a multitude of natural products. The most obvious FXR modulators are compounds with a steroidal structure, like the triterpene oleanolic acid, as this structure closely resembles the endogenous agonists. However, there are also other structural classes among FXR agonists like the sesquiterpene alcohol farnesol that gave FXR its name or the polyphenols xanthohumol and epigallocatechin gallate [5, 12].

Leoligin, the major lignan from the roots of *L. nivale* ssp. *alpinum*, is reported to influence cholesterol metabolism via cholesteryl ester transfer protein (CETP), 3-hydroxy-3-methyl-glutaryl-CoA reductase (HMGCR), and ATP-binding cassette transporters A1 (ABCA1) and G1 (ABCG1) [13–15], and is thus an interesting candidate for FXR modulation. In context of an interdisciplinary research program [16] exploiting natural compound isolates towards new potential drug leads [17], we established a stereoselective synthetic route for the generation of a compound library based on the leoligin core structure [18]. In order to identify potential and novel FXR agonists, we utilized FXR specific pharmacophore models [19] to screen a database of leoligin structural analogs. Selected virtual hits were tested in a cell-based FXR transactivation assay and yielded 7 FXR activating compounds, the most promising termed LT-141A. Furthermore, we characterized this novel FXR agonist for its effects on cholesterol metabolism in human cell models for macrophage cholesterol efflux and intestinal cholesterol uptake.

Results

All pharmacophore models reported in reference [19] were used to screen 168 synthetic leoligin analogs (► **Fig. 1 a**). Nearly all compounds fitted into the FXR ligand models 3fli-1 and 3fli-1-s (► **Fig. 2**), which pointed towards this compound class as interesting test substances. Fifty-nine compounds were predicted by at least 1 additional model.

To validate the *in silico* predictions, 65 virtual hits, preferably those found by 3fli- and additional models, were tested in a cell-based FXR transactivation assay. This yielded 7 FXR activating compounds, with the most active one being LT-141A (► **Fig. 1 b** and **Table 1**). LT-141A concentration-dependently transactivated FXR with an EC₅₀ of 6.36 µM and an E_{max} of 4.1-fold compared to

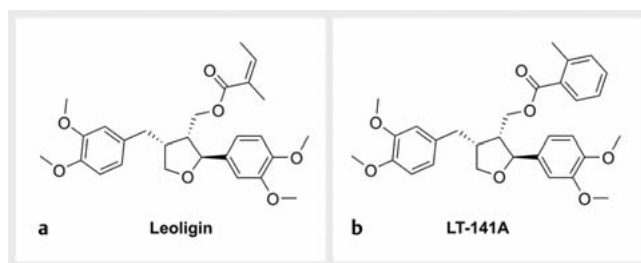
the vehicle control in a transactivation assay using the bile salt export pump (BSEP) promoter coupled to a luciferase gene. Interestingly, LT-141A showed a similar response as the endogenous FXR agonist CDCA (► Fig. 3a). We also compared LT-141A to its parent compound leoligin in the same assay. Leoligin only slightly increased FXR transactivation with an E_{\max} of 1.5-fold compared to the vehicle control (► Fig. 3b). Taken together, this strong increase in FXR transactivation was achieved by the exchange of the angelic acid ester of leoligin with an in *o*-position methylated benzoic acid ester (► Fig. 1).

In order to investigate if, in addition to its agonistic properties, LT-141A can act as an antagonist, we determined the reduction in CDCA-induced FXR activity in a full-length receptor transactivation assay. In this assay, LT-141A was able to reduce CDCA-induced FXR activity to 59.45%, thereby showing clear antagonistic properties (► Fig. 3c).

To better understand if LT-141A can either directly or indirectly activate FXR, we performed an FXR-Gal4 assay. In this assay, LT-141A showed an EC_{50} of 5 μ M and E_{\max} of 14.2-fold compared to the vehicle control (► Fig. 4a), whereas leoligin had a marginal effect with an E_{\max} of 1.4-fold compared to the vehicle control (► Fig. 4b). In addition, LT-141A reduced CDCA-induced FXR-Gal4 activity to 44.11% (► Fig. 4c). Furthermore, we performed FXR binding pose predictions with CDCA and LT-141A, showing that the residues Arg331 and Ser332 are particularly important for LT-141A binding (► Fig. 5).

To further strengthen the assumption that LT-141A binds to the FXR ligand binding domain (LBD), we performed an FXR co-activator assay. LT-141A successfully recruited the co-activator peptide SRC2-2 to the FXR LBD with an EC_{50} of 2.5 μ M (► Fig. 4d). The endogenous full FXR ligand CDCA recruited SRC2-2 with an EC_{50} of 12.7 μ M but with much higher affinity, further illustrating the partial agonistic nature of LT-141A. Next, we evaluated the selectivity of LT-141A toward the nuclear receptors retinoid X receptor α (RXR α), the liver X receptors α and β (LXR α and β), the peroxisome proliferator-activated receptor β/δ , and γ (PPAR β/δ , and γ) and the G-protein coupled bile acid receptor TGR5 (GPBAR1), all of which are involved in the regulation of metabolic processes. We used cell-based transactivation assays to determine activities on the mentioned receptors. Interestingly, LT-141A was not able to activate any of the tested receptors (Supplementary Fig. 1S, Supporting Information).

To study the consequences of FXR activation, we investigated a direct and indirect FXR target gene in the liver cell line HepG2. Induction of small heterodimer partner (SHP), a bona-fide FXR target gene, is a major mechanism to suppress gene expression [20]. SHP mRNA expression was significantly increased by the FXR agonist GW4064 as expected, and also LT-141A increased its expression significantly between 30 and 1 μ M, although not concentration-dependently (► Fig. 6a). CYP7A1 is an indirect FXR target gene, downregulated via SHP, and a key enzyme in bile acid synthesis. Upon FXR activation, this gene is downregulated as observed with GW4064. LT-141A, however, had no effect on the expression of the CYP7A1 gene when compared to vehicle control (► Fig. 6b). We also investigated the mRNA expression levels of the FXR target gene fibroblast growth factor 19 (FGF19) in intestinal Caco-2 cells. GW4064 significantly upregulated this gene, however, only around



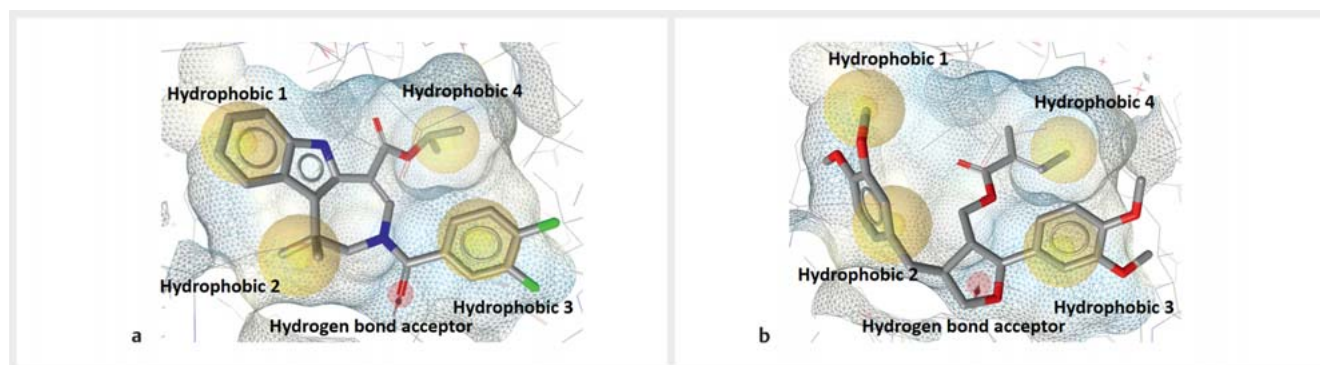
► Fig. 1 Chemical structures of leoligin and LT-141A.

2-fold. The weaker endogenous FXR agonist CDCA and LT-141A had no effect on the mRNA of this target gene (► Fig. 6c).

In order to evaluate a putative effect of LT-141A on cholesterol homeostasis, we investigated its influence on cholesterol uptake in intestinal Caco-2 cells. A decreased uptake of cholesterol in these cells implies a lower systemic cholesterol burden and a higher fecal cholesterol excretion, making it beneficial especially for metabolic diseases. As a positive control the LXR agonist GW3965 was used, which significantly decreased cholesterol uptake. LT-141A showed a comparable effect to GW3965, whereas the 2 FXR agonists CDCA and GW4064 did not elicit a significant decrease (► Fig. 7a). Next, we investigated LT-141A's influence on ApoA1-mediated cholesterol efflux in THP1-derived macrophages. Cholesterol efflux from macrophages is an important mechanism in the prevention of atherosclerosis *via* inhibition of foam cell formation. LT-141A at 10 μ M increased cholesterol efflux approximately 2.5-fold, being even stronger than the positive control pioglitazone (10 μ M), a PPAR γ agonist (► Fig. 7b). Investigation of the responsible mechanism behind the increased cholesterol efflux from macrophages revealed that not only the mRNA (► Fig. 7c) but also the protein level (► Fig. 7d) of the cholesterol transporter ABCA1 is dose-dependently elevated upon treatment with LT-141A, suggesting a direct link. Interestingly, CDCA but not GW4064 significantly increased ABCA1 mRNA levels (► Fig. 7c). As ABCA1 is not only an important cholesterol transporter in macrophages but also in intestinal and liver cells, we measured ABCA1 protein levels in these cell types. The positive controls GW3965 and T0901317, 2 LXR agonists, significantly increased ABCA1 protein in both cell types, as expected. However, LT-141A as well as the FXR agonists GW4064 and CDCA had no effect on ABCA1 protein expression (► Fig. 7e and f). These results suggest a cell type-specific effect of LT-141A that seems to be only partially dependent on FXR activation.

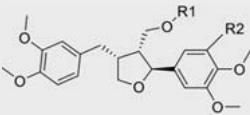
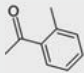
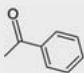
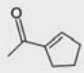
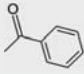
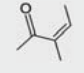
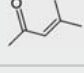
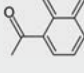
Discussion

In the present study, we identified a novel SBARM, LT-141A, that had no cross-activity on other metabolic nuclear receptors (PPARs, LXR α/β , and RXR) and, more importantly, did not activate TGR5 (GPBAR1). Off-target effects of FXR modulators often include the activation of this bile acid responsive G-protein coupled receptor. TGR5 activation is a possible reason for the occurrence of pruritus, besides other molecular causes, which is the most common reason for treatment discontinuation of FXR agonists in patients.



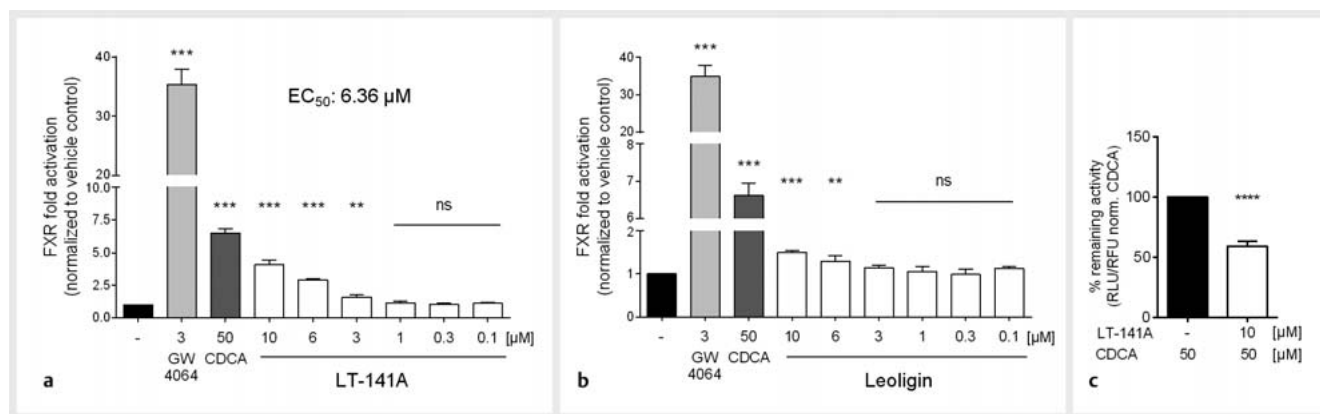
► **Fig. 2** Pharmacophore-based virtual screening. A structure-based pharmacophore model for FXR agonists based on the PDB entry 3fli [31] mapped the majority of leoligin analogs from a virtual library. **a** The co-crystallized FXR agonist XL335 (WAY-362450) with 4 hydrophobic contacts (yellow spheres) and a hydrogen bond acceptor (red arrow) anchoring the compound in the binding site. **b** Leoligin matching the 5 pharmacophore features of the 3fli-based model.

► **Table 1** Leoligin analogs identified as FXR modulators.

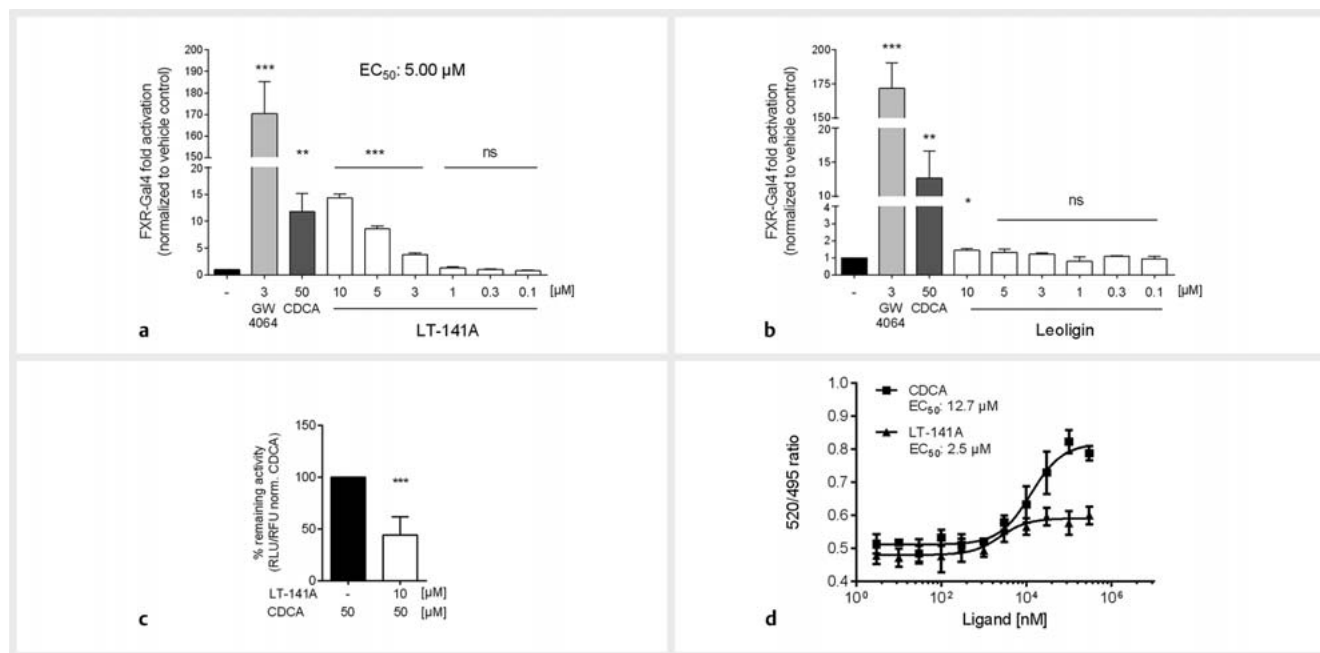
|  common structure | | | | |
|---|---|------------------|-------------------------------|--|
| Compound ID | R1 | R2 | Fold activation at 10 μ M | |
| LT-141A |  | H | 4.79 \pm 0.92 | |
| LT-071A |  | H | 3.75 \pm 0.13 | |
| LT-095A |  | H | 2.44 \pm 0.49 | |
| SOGE-21 |  | OCH ₃ | 2.23 \pm 0.37 | |
| Leoligin |  | H | 1.84 \pm 0.28 | |
| LT-075A1 |  | H | 1.81 \pm 0.23 | |
| LT-104A |  | H | 1.56 \pm 0.16 | |

Leoligin, a lignan-type secondary metabolite, originally isolated from the roots of the alpine plant *L. nivale* ssp. *alpinum* has been reported to reduce cholesterol levels and inhibit HMGCR in ApoE^{-/-} mice, to activate CETP *in vivo* and *in vitro*, and to promote

cholesterol efflux from human THP1-derived macrophages *via* up-regulation of the cholesterol transporters ABCA1 and ABCG1 [13–15]. These overall favorable *in vivo* and *in vitro* properties on cholesterol metabolism encouraged us to use leoligin as parent com-



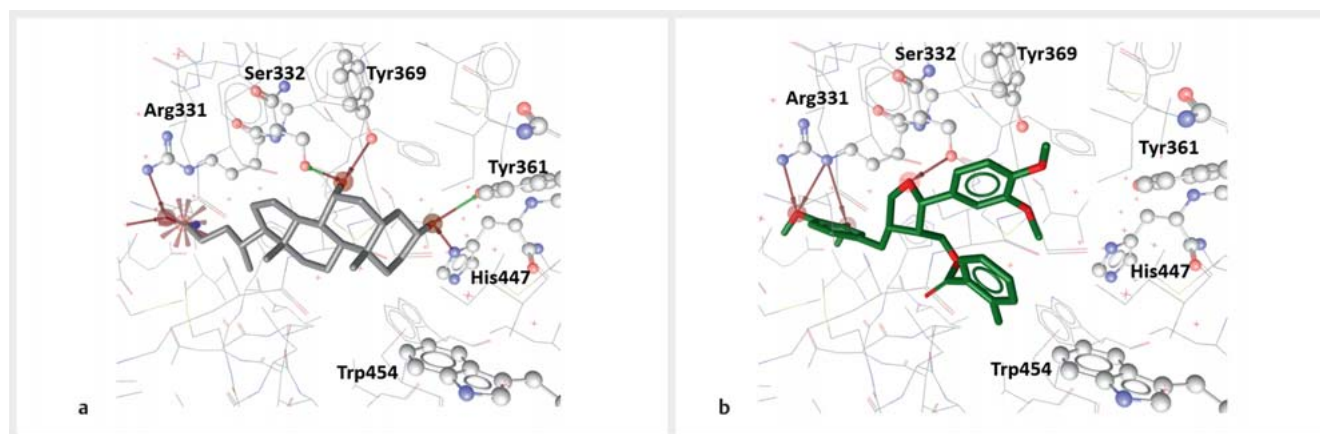
► **Fig. 3** Concentration-dependent FXR transactivation by LT-141A and leoligin. HEK-293 cells were cotransfected with an hFXR expression plasmid, a BSEP luciferase reporter plasmid, and an EGFP plasmid as internal control. Cells were treated with 3 μM GW4064 and 50 μM CDCA as positive control or the indicated concentrations of (a) LT-141A, (b) leoligin for 18 h, or (c) CDCA for 18.5 h and LT-141A for 18 h. The measured luciferase-derived luminescence was normalized to the obtained EGFP-derived fluorescence and to the vehicle control. Each bar represents the mean ± SD of at least 3 independent experiments performed in quadruplicate and evaluated by 1-way ANOVA with the Bonferroni post-test or Student's t-test. **** p < 0.0001, *** p < 0.001, ** p < 0.01 compared with vehicle control (DMSO), ns not significant versus DMSO.



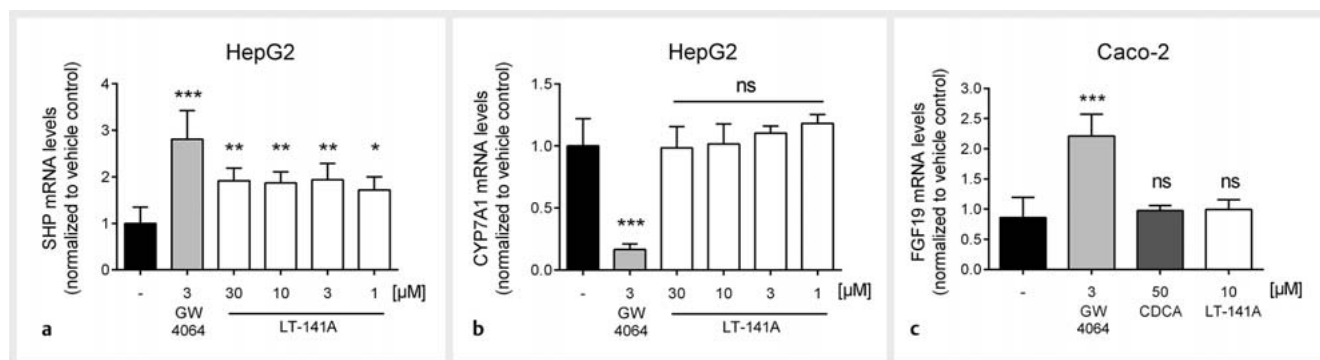
► **Fig. 4** Concentration-dependent FXR-Gal4 transactivation by LT-141A and leoligin. HEK-293 cells were cotransfected with an FXR-Gal4 plasmid, tk(MH1000)4xLuc luciferase reporter plasmid and an EGFP plasmid as internal control. Cells were treated with 3 μM GW4064 and 50 μM CDCA as positive control or the indicated concentrations of (a) LT-141A, (b) leoligin for 18 h, or (c) CDCA for 18.5 h and LT-141A for 18 h. The measured luciferase-derived luminescence was normalized to the obtained EGFP-derived fluorescence and to vehicle control. Each bar represents the mean ± SD of at least 3 independent experiments performed in quadruplicate and evaluated by 1-way ANOVA with the Bonferroni post-test or Student's t-test. *** p < 0.001, * p < 0.05 compared with vehicle control (DMSO), ns not significant versus DMSO. **d** A Lanthascreen TR-FRET FXR Co-activator assay was performed with LT-141A and CDCA in various concentrations. Results represent 4 experiments performed in quadruplicates.

pound to identify new FXR modulators. For this purpose, we used a previously synthesized library of 168 leoligin analogs [18] that were screened in an *in silico* structure-based pharmacophore model. LT-141A was able to potently activate FXR in a transactivation assay and bind the FXR ligand-binding domain in a Gal4-based assay with EC₅₀ values of 6.36 μM and 5 μM, respectively.

Additionally, LT-141A was active in an FXR co-activator recruitment assay with an EC₅₀ of 2.5 μM. Compared to the endogenous full FXR agonist CDCA, LT-141A showed a lower affinity to the co-activator peptide SRC2-2, thereby indicating partial agonism and binding to the FXR LBD. Leoligin, on the other hand, had no or only marginal influence in the Gal4-based assay. This particular



► **Fig. 5** FXR binding pose prediction for LT-141A. a Binding pose of the positive control CDCA in the human FXR co-crystal structure (PDB code 6hl1). b Predicted binding pose of LT-141A in the same structure. Electrostatic anchoring via hydrogen bonds (arrows) and charged interactions (star) are depicted for comparison.



► **Fig. 6** Influence of LT-141A on the expression of different FXR target genes. HepG2 cells were treated with the indicated test substances for 24 h. The mRNA levels of (a) SHP and (b) CYP7A1 were detected by RT-qPCR. c Differentiated Caco-2 cells were treated with the indicated test substances for 24 h. The mRNA levels of FGF19 were detected by RT-qPCR. Bar graphs represent mean \pm SD from at least 3 independent experiments, evaluated by 1-way ANOVA with the Bonferroni post-test or Student's t-test. *** p < 0.001, ** p < 0.01, * p < 0.05 compared with vehicle control (DMSO), ns not significant versus DMSO.

change in pharmacological activity seems to be an immediate consequence of the significant structural change from an olefinic to an aromatic ester group within the leoligin scaffold. In addition, LT-141A reduced CDCA-induced FXR activity in FXR transactivation and Gal4 assays. These results corroborate the partial agonism of LT-141A and are in line with the observation that some partial FXR agonists cause a structural conformation able to bind co-activator and co-repressor peptides [11].

Target gene expression studies revealed that LT-141A does not act as a classical agonist, but as a SBARM. CYP7A1, a key enzyme in bile acid biosynthesis, is downregulated by FXR agonists like GW4064. LT-141A, however, did not change the expression level of this gene. Another direct target gene of FXR is FGF19. FGF19 is expressed in intestinal cells and secreted to reach the liver, where it regulates gene expression. FXR agonists upregulate this gene; however, LT-141A had no effect on FGF19 mRNA levels in Caco-2 cells. The reason for this might be the general low response of FXR agonists on this gene in our experimental setting. SHP, on the other hand, was upregulated with LT-141A as with the FXR agonist

GW4064. These results clearly show that LT-141A acts as a gene-selective FXR agonist.

FXR is a key regulator of bile acid biosynthesis and therefore also a major player in cholesterol metabolism. This prompted us to investigate the effect of LT-141A in functional settings for cholesterol homeostasis. Cholesterol uptake from dietary sources occurs in the intestine. A reduced intestinal cholesterol uptake corresponds to a reduced systemic cholesterol load and is therefore beneficial in the therapy of metabolic syndrome-related diseases. Remarkably, LT-141A reduced the cholesterol uptake to a similar extent as the LXR agonist GW3965, whereas the FXR agonists CDCA and GW4064 had no effect. The FXR agonistic property of LT-141A seems therefore not to be responsible for the decreased cholesterol uptake in Caco-2 cells.

We additionally examined if LT-141A can increase cholesterol efflux from macrophages. This would suggest an anti-atherosclerotic effect as accumulation of cholesterol in macrophages leads to the formation of foam cells, which are a major indicator for the development of atherosclerotic plaques. LT-141A increased ApoAI-

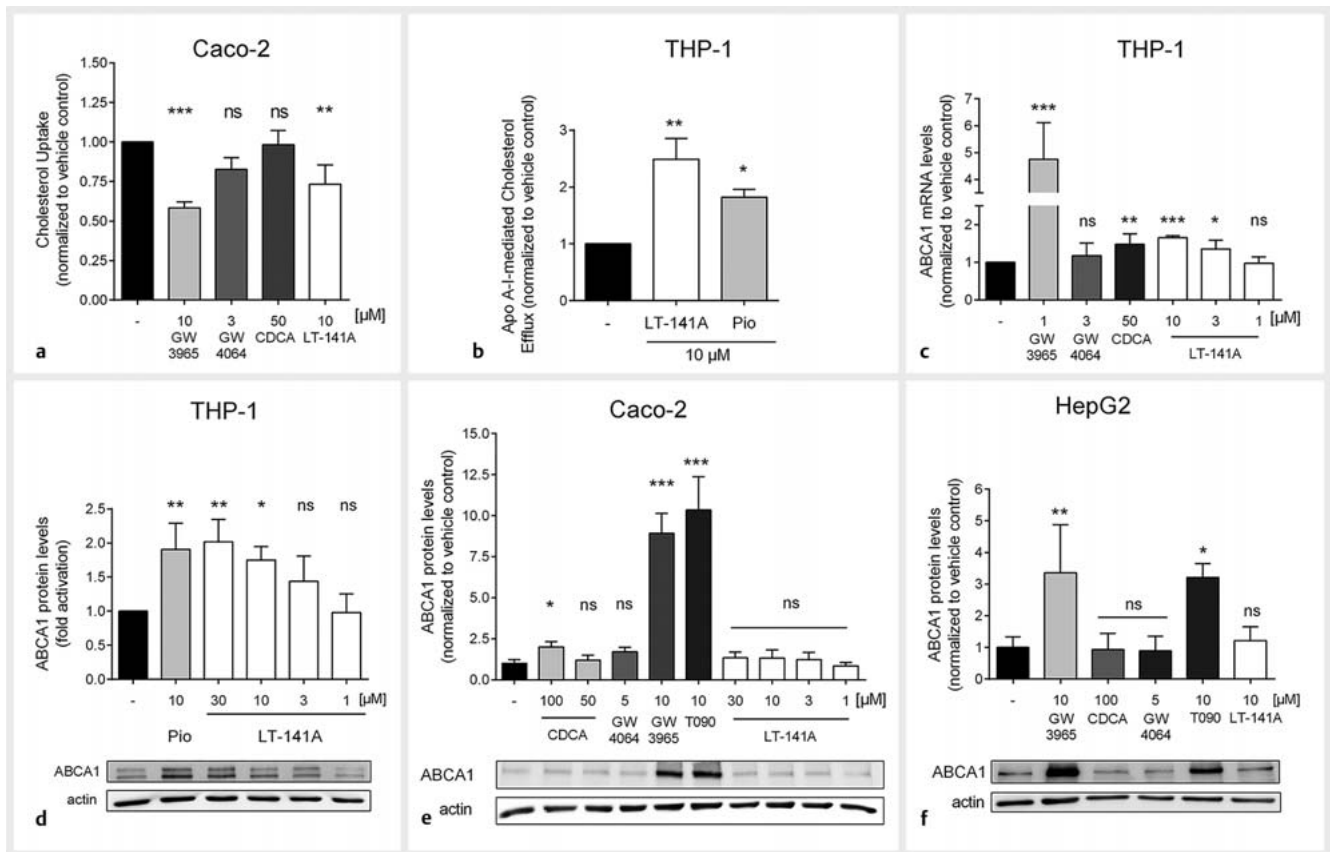


Fig. 7 LT-141A regulates cholesterol transport. **a** Cholesterol uptake in intestinal Caco-2 cells was determined as described in the material and methods section. **b** Cholesterol efflux from THP1-macrophages was determined as described in the material and methods section. **c** THP1-macrophages were treated with the indicated test substances for 24 h. The mRNA levels of ABCA1 were detected by RT-qPCR. **d** THP1-macrophages were treated with the indicated test substances for 24 h. The ABCA1 protein levels were detected by western blot. **e** Differentiated Caco-2 cells were treated with the indicated test substances for 48 h. The ABCA1 protein levels were detected by western blot. **f** HepG2 cells were treated with the indicated test substances for 24 h. The ABCA1 protein levels were detected by western blot. Bar graphs represent mean \pm SD from at least 3 independent experiments, evaluated by 1-way ANOVA with the Bonferroni post-test or Student's t-test. *** p < 0.001, ** p < 0.01, * p < 0.05 compared with vehicle control (DMSO), ns not significant versus DMSO.

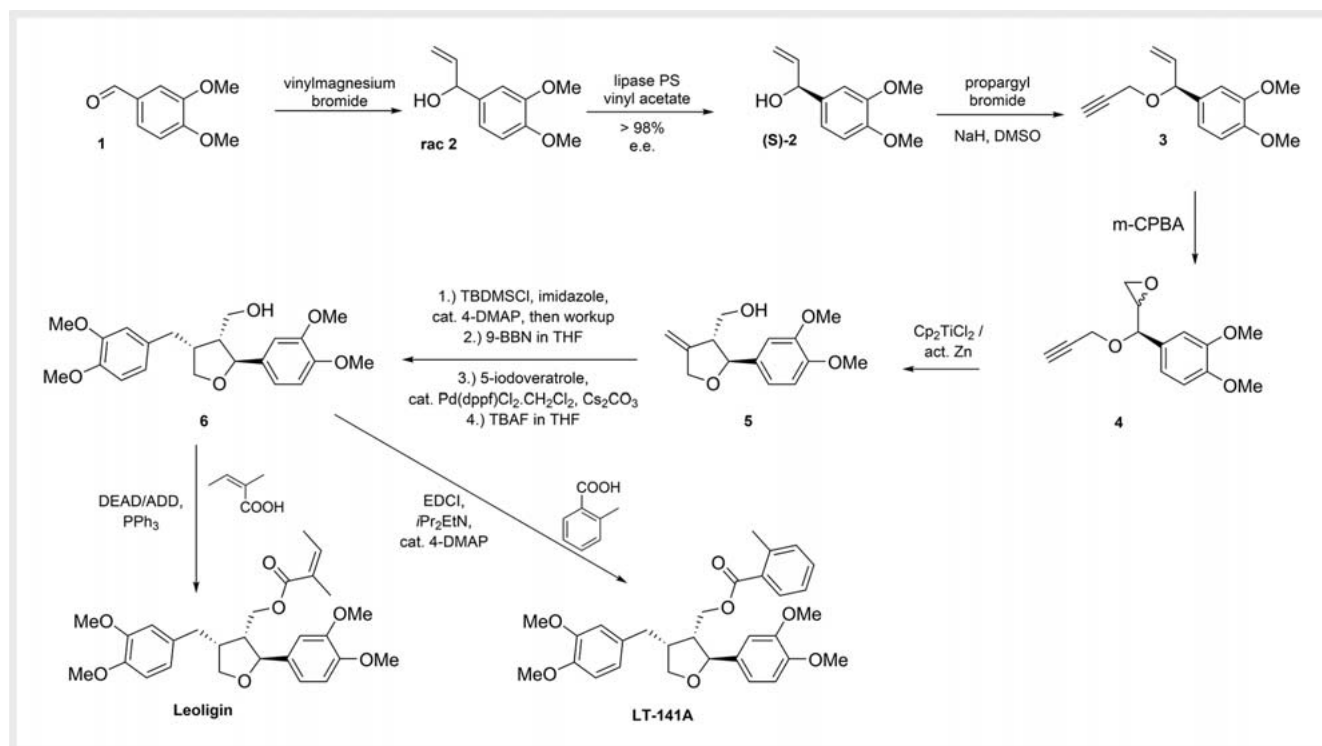
mediated macrophage cholesterol efflux even stronger than the PPAR γ agonist pioglitazone. PPAR γ increases cholesterol efflux *via* the induction of LXR expression [21,22]. Increased expression of the well-studied cholesterol transporter ABCA1 seems to be responsible for the enhanced cholesterol efflux upon treatment with LT-141A. Interestingly, GW4064 did not increase ABCA1 mRNA levels, but CDCA did, pointing to a different mechanism underlying cholesterol efflux than FXR agonism. In the liver cell line HepG2, ABCA1 expression is, however, neither influenced by the FXR agonists, GW4064 or CDCA, nor by LT-141A. A similar pattern was observed in the intestinal cell line Caco-2, where neither the FXR agonist GW4064 nor LT-141A had an effect on ABCA1 mRNA levels. CDCA slightly upregulated ABCA1 mRNA in this setting, suggesting again an alternative mechanism of ABCA1 regulation. The LXR agonists GW3965 and T0901317 increased ABCA1 levels in all tested cell types as is suggested by literature [23–26].

It is kind of puzzling that LT-141A is not activating LXR as it clearly upregulated the expression of the LXR target gene ABCA1 in macrophages. Also, the FXR agonist GW4064 did not mimic the effects of LT-141A on ABCA1 mRNA expression, but CDCA did. As

ABCA1 expression can be regulated at the transcriptional, post-transcriptional, and post-translational level, a plethora of possible mechanisms exists for the induction of both ABCA1 mRNA and protein expression by LT-141A.

All the obtained results not only suggest target-gene but also cell-type selectivity of LT-141A. Such tissue-selective FXR agonists may provide a beneficial side effect profile and are therefore interesting for the development of novel drugs. Tissue-specificity could be achieved *via* differential availability of transporters or by reducing the retention time of a substance in a specific tissue. Moreover, differential expression of co-regulatory proteins in these cell types might lead to tissue-specific target gene expression. Several intestinal-specific FXR agonists are already known (fexaramine, TC-100, ivermectin, ECGC) and are suggested to be safer for the treatment of metabolic syndrome-related diseases than systemic FXR agonists [8].

Taken together, we could identify a novel FXR agonist, LT-141A, with an EC_{50} of 6.36 μ M in an FXR transactivation assay and 5 μ M in an FXR-Gal4 assay, without activating other metabolic nuclear receptors and the G-protein coupled bile acid receptor



► Fig. 8 Synthesis pathway for leoligin and LT-141A.

TGR5. LT-141A has been shown to enhance cholesterol efflux from THP-1-derived macrophages via upregulation of the cholesterol transporter ABCA1. Additionally, LT-141A also decreased cholesterol uptake in intestinal cells. These results display potential beneficial effects of LT-141A on cholesterol metabolism and characterize LT-141A as target gene and cell-type selective FXR agonist.

Materials and Methods

Synthesis of leoligin and leoligin analogs

A synthetic route for the total synthesis of leoligin (► Fig. 8), which can be applied as well for synthesizing leoligin analogs has been established previously [18]. Standard addition of vinylmagnesium bromide to **1** delivered the substrate for the first key step of our synthesis: establishing chirality upon lipase-mediated kinetic resolution of **rac-2** to **(S)-2** employing Amano lipase PS in high optical purity. The further synthesis consisted of etherification of **(S)-2** to **3**, followed by standard *m*-CPBA epoxidation to **4**. Subsequent radical cyclization [27,28] delivered the tetrahydrofuran scaffold **5**. Noteworthy, the synthesis of **5** from **(S)-2** could be carried out in a single operation without isolation of intermediates **3** and **4**. The hydroxymethyl group in intermediate **5** was protected with the sterically demanding TBDMS group since its steric bulk ensures 3,4-*cis* diastereoselective hydroboration with commonly used 9-borabicyclo(3.3.1)nonane (9-BBN) as reagent. The hydroboration product was again not isolated but subjected *in situ* to a Suzuki-Miyaura coupling with 5-iodoveratrole to deliver **6** after concomitant deprotection. A final esterification of the hy-

droxy group with either angelic acid or 2-methylbenzoic acid delivered leoligin and LT-141A, respectively. By varying the aryl halide coupling partner in the Suzuki-Miyaura step and the carboxylic acid in the esterification, a library of leoligin analogs can be synthesized. Details for all reaction steps and analytical data of all compounds can be found in the Supporting Information.

Pharmacophore-based virtual screening

Pharmacophore-based virtual screening was performed using DiscoveryStudio version 2015 (BIOVIA, Dassault Systèmes Discovery Studio Modeling Environment: Dassault Systèmes, 2015). From the 2D structures of 168 leoligin analogs, a 3D multi-conformational database was calculated with a maximum of 500 conformers per molecule using BEST conformational analysis settings. This database was screened against a previously established FXR ligand pharmacophore model set [19] using BEST FLEXIBLE fitting. This means that the screening ligand conformation is energetically minimized during the pharmacophore matching so that it better fits into the model.

Cell culture reagents, chemicals, and plasmids

DMEM, containing 4.5 g/L glucose, L-glutamine, Eagle's minimum essential medium (EMEM) without L-glutamine, RPMI-1640, non-essential amino acids, benzylpenicillin, and streptomycin were obtained from Lonza. FBS and trypsin was supplied by Gibco *via* Invitrogen. Phorbol 12-myristate 13-acetate (PMA), water-soluble cholesterol, ApoA1, sodium taurocholate, lysophosphatidylcholine, oleic acid, monooleoylglycerol, GW4064 (purity ≥ 97%), CDCA (purity ≥ 96%), GW3965 (purity ≥ 98%), pioglitazone (purity ≥ 98%), lithocholic acid (purity ≥ 95%), and T0901317 (purity

≥ 98 %) were purchased from Sigma-Aldrich. Fatty acid-free bovine serum albumin (BSA) was obtained from Carl Roth. [³H]-cholesterol was provided by PerkinElmer. Human plasma was obtained from young, healthy volunteers.

The hFXR expression plasmid, the bile salt export pump (BSEP)-Luc plasmid, and the FXR-Gal4 plasmid were kindly provided by Prof. Dr. Schubert-Zsilavecz (Goethe University Frankfurt). The PPAR luciferase reporter construct (tk-PPREx3-luc) and the reporter plasmid for the Gal4 assay (tk(MH1000)4xLuc) was a kind gift from Prof. Ronald M. Evans (Howard Hughes Medical Institute). The expression plasmids for human PPAR subtypes (pSG5-hPPAR- β , pSG5-PL-hPPAR- γ 1) were a kind gift from Prof. Walter Wahli and Prof. Beatrice Desvergne (Center for Integrative Genomics, University of Lausanne). The ABCA1-Luc Plasmid was kindly provided by Prof. Ira G. Schulman (University of Virginia). The human RXR α , LXR α , and β expression plasmids were bought from Missouri S&T cDNA Resource Center and the RXRE-Luc plasmid from Panomics. The TGR5 expression plasmid, GPBAR1, transcript variant 3, NM_170699.1 (OG-SC123315) was obtained from Origene via Biomedica. The CRE-Luc plasmid, pGL4.29[luc2P/CRE/Hygro], was obtained from Promega. The plasmid encoding enhanced green fluorescence protein (pEGFP-N1) was obtained from Clontech.

The primary antibody against ABCA1 (catalog no. NB400-105) was obtained from Novus Biologicals. The anti-actin antibody (catalog no. 8691002) was acquired from MP Biologicals. Goat antimouse secondary antibody, HRP conjugate (catalog no. 12-349), was purchased from Millipore, and antirabbit IgG, HRP-linked secondary antibody (catalog no. 7074S), was obtained from Cell Signaling via New England Biolabs. The peqGOLD Total RNA Kit was purchased from PeqLab, and the High Capacity cDNA Reverse Transcription Kit was from Applied Biosystems. The LightCycler 480 SYBR Green I Master was purchased from Roche. ABCA1 (Hs_ABCA1_1_SG QuantiTect Primer Assay, catalog no. QT00064869), CYP7A1 (Hs_CYP7A1_1_SG QuantiTect Primer Assay, catalog no. QT00001085), SHP (Hs_NR0B2_1_SG QuantiTect Primer Assay, catalog no. QT00061460), GAPDH (Hs_GAPDH_1_SG QuantiTect Primer Assay, catalog no. QT00079247), FGF19 (Hs_FGF19_2_SG QuantiTect Primer Assay, catalog no. QT02452289), and BSEP (Hs_ABCB11_1_SG QuantiTect Primer Assay, catalog no. QT00035049) oligonucleotide primers were purchased from Qiagen.

Luciferase reporter gene assays

For the luciferase reporter gene assays, HEK-293 cells (ATCC) were maintained in DMEM containing 4.5 g/L glucose supplemented with 2 mM L-glutamine, 10% FBS, 100 U/mL benzylpenicillin, and 100 μ g/mL streptomycin. Cells were grown in 15 cm dishes at a density of 6×10^6 cells per dish for 19 h and then transfected *via* the calcium phosphate precipitation method. After 6 h, the cells were reseeded to 96-well plates (5×10^4 cells/well) in DMEM containing 4.5 g/L glucose supplemented with 2 mM L-glutamine, 100 U/mL benzylpenicillin, 100 μ g/mL streptomycin, and 5% charcoal-stripped FBS. Cells were treated with indicated concentrations of test compounds, positive control (50 μ M CDCA and 3 μ M GW4064 for FXR, 1 μ M GW3965 for LXR α / β , 10 nM GW0742 for PPAR β / δ , 10 μ M pioglitazone for PPAR γ , and 10 μ M lithocholic acid for TGR5) or solvent vehicle (0.1% DMSO) and incubated for 18 h.

Cells were then lysed and the luminescence of the firefly luciferase and the fluorescence of EGFP were quantified with a Tecan Spark plate reader. The luciferase-derived luminescence was normalized to the EGFP-derived fluorescence from each well to account for differences in transfection efficiency or cell number. For the FXR transfections, 5 μ g hFXR or 1 μ g FXR-Gal4 plasmid, 5 μ g reporter plasmid (BSEP-Luc plasmid or tk(MH1000)4xLuc plasmid, respectively) were used. For the RXR α , LXR α / β , PPAR γ transfections, 6 μ g expression plasmid and 6 μ g reporter plasmid (RXRE-Luc, ABCA1-Luc, and PPRE-Luc, respectively) were used. For the PPAR β / δ transfection, 1 μ g expression plasmid and 6 μ g reporter plasmid were used. For the TGR5 transfection, 5 μ g expression plasmid and 5 μ g CRE-reporter plasmid were used. As internal control, 3 μ g EGFP plasmid was transfected in all assays.

LanthaScreen TR-FRET FXR co-activator assay

The LanthaScreen TR-FRET FXR Co-activator Assay Kit (Invitrogen) was used according to the manufacturer's instructions. In short, GST-tagged FXR LBD is added to varying concentrations of LT-141A and CDCA (300 μ M–3 nM). Then the fluorescein-labeled SRC2-2 co-activator peptide and terbium-labeled anti-GST antibody is added in a 384-well plate to a total volume of 20 μ l. After 1 h of incubation at room temperature, fluorescence was measured at 520 nm and normalized to the fluorescence measured at 495 nm (Tecan Spark). The 520 nm/495 nm ratios were used to determine the binding of the test compounds to the FXR LBD.

THP-1, HepG2, and Caco-2 cell culture

THP-1 cells were obtained from ATCC and maintained in RPMI-1640 medium supplemented with 10% heat-inactivated FBS, 100 U/mL penicillin, 100 μ g/mL streptomycin, and 2 mM L-glutamine at 37 °C in an incubator with 5% CO₂. THP-1 macrophages were acquired upon stimulation with 200 nM PMA for 72 h. HepG2 cells (ATCC) were maintained in DMEM medium supplemented with 10% heat-inactivated FBS, 100 U/mL penicillin, 100 μ g/mL streptomycin, and 2 mM L-glutamine at 37 °C in an incubator with 5% CO₂. Caco-2 cells were obtained from DSMZ and maintained in EMEM medium supplemented with 20% heat-inactivated FBS, 2 mM L-glutamine, and 1 \times nonessential amino acids at 37 °C in an incubator with 5% CO₂. Test substances were dissolved in dimethyl sulfoxide (DMSO). The final DMSO concentration in all experiments was equal to 0.1%.

RNA extraction and reverse transcription-quantitative polymerase chain reaction (RT-qPCR)

THP-1 cells were seeded at a density of 0.2×10^6 /mL in a volume of 4 mL per well in 6-well plates and differentiated for 72 h, then loaded with cholesterol (10 μ g/ml) and treated with the indicated test substances for 24 h, as described previously [15]. After treatment, total RNA was extracted from cells using the peqGOLD Total RNA Kit. Concentration of total RNA was measured with NanoDrop 2000c. cDNA was synthesized from 1 μ g total RNA based on the protocol from the High Capacity cDNA Reverse Transcription Kit. In combination with the LightCycler 480 System from Roche, LightCycler 480 SYBR Green I Master was used for quantification of mRNA expression. Relative mRNA levels were quantified with the Δ CT method, using human GAPDH as an en-

dogenuous control. HepG2 cells were seeded at a density of 1×10^6 /mL in 6-well plates. After 24 h, cells were treated in DMEM supplemented with 5% stripped FBS, 2 mM L-glutamine, 100 U/mL penicillin, and 100 µg/mL streptomycin with test substances for another 24 h. Total RNA extraction and RT-qPCR were performed like for THP-1 cells. Caco-2 cells were seeded at 0.06×10^6 cells/cm² on PET transwell inserts (Sarstedt) and cultivated for 19 days under asymmetric conditions (EMEM with L-glutamine, streptomycin, penicillin, and non-essential amino acids on the apical side and the same medium with additional 20% heat-inactivated FBS on the basolateral side). Transepithelial electrical resistance measurements were routinely performed to evaluate the integrity of the cell monolayer. After 19 days, the medium was changed to serum-free medium in the apical and medium supplemented with 0.5% BSA on the basolateral compartment for 24 h. After that, cells were treated with test compounds for another 24 h. Total RNA extraction was performed with the TRIzol reagent from Invitrogen. RT-qPCR was performed as described for THP-1 cells. GAPDH was used as housekeeping gene.

Western blot analysis

THP-1 macrophages, Caco-2 cells, or HepG2 cells were prepared as described for RNA extraction. THP-1 macrophages and HepG2 cells were treated for 24 h with the indicated substances and Caco-2 cells for 48 h. Cells were washed with cold PBS (4°C) and lysed with NP40 buffer (THP-1, Caco-2; 150 mM NaCl; 50 mM HEPES (pH 7.4); 1% NP40) or RIPA buffer (HepG2; 500 mM NaCl; 50 mM TrisHCl pH 6.8; 1% Nonidet P40; 0.5% deoxycholat; 0.1% SDS; 0.05% sodium azide), respectively, containing a protease inhibitor mixture (1% Complete (Roche); 1% phenylmethylsulfonyl fluoride; 0.5% Na₃VO₄; 0.5% NaF). Cell lysates were harvested and centrifuged at 16000 g for 20 min at 4°C to remove cell debris. Protein concentration was determined by the Bradford method. An equal amount of protein samples was resolved *via* sodium dodecyl sulfate-polyacrylamide gel electrophoresis (SDS-PAGE) and then transferred onto a PVDF membrane (Bio-Rad). The membranes were blocked with 5% low-fat milk and sequentially incubated with the primary antibodies [ABCA1 (1:500); actin (1:5000)] and appropriate secondary antibodies [goat antimouse secondary antibody, HRP conjugate (1:5000) or antirabbit IgG, HRP-linked secondary antibody (1:500)] according to the manufacturer's instructions. Luminescence was detected after incubation with ECL-reagent by a LAS-3000 (Fujifilm). Densitometric analysis was performed using the Multi Gauge software (Fujifilm). Actin protein levels were used as loading control.

Cholesterol uptake in intestinal Caco-2 cells

Caco-2 cells were prepared as described for RNA extraction. They were treated for 48 h with the indicated test substances. Cells were then washed with PBS and 1.8 mL of serum-free DMEM supplemented with 2 mM L-glutamine, 1× nonessential amino acids, and 1% human plasma was added to the basolateral compartment. A micellar solution containing 0.05 mM cholesterol, 1 µCi/mL [3H]-cholesterol, 2 mM sodium taurocholate, 0.2 mM lyso-phosphatidylcholine, 0.6 mM oleic acid, and 0.2 mM monooleoyl-glycerol, together with test substances, was added to the apical compartment and incubated for 2 h at 37°C on the orbital shaker

(200 rpm). Cells were then lysed with NP40 lysis buffer (150 mM NaCl; 50 mM HEPES (pH 7.4); 1% NP40). The radioactivity in these lysates was then measured by liquid scintillation counting. Cholesterol uptake was calculated by normalization to protein content as determined by the Bradford method.

Cholesterol efflux from THP-1-derived macrophages

Cellular cholesterol efflux was measured as previously described [29]. In short, THP-1 cells were seeded at a density of 0.2×10^6 /mL per well in 24-well plates and differentiated for 72 h. After being washed twice with PBS, macrophages were treated with test substances and labeled by incubation in RPMI-1640 medium supplemented with 2.5% FBS, [3H]-cholesterol (0.5 µCi/mL), and cholesterol (10 µg/mL). Cells were washed with PBS and then incubated with fresh serum-free medium containing 10 µg/mL ApoA1 for 6 h to induce macrophage cholesterol efflux. Effluxed (supernatant) and intracellular (cell lysate) [3H]-cholesterol was counted by liquid scintillation. Cholesterol efflux (percentage of total cholesterol) was determined by the ratio of radio-labeled cholesterol in the supernatant to that of both supernatant and cells. The specific efflux is calculated as the difference between the efflux in the presence and absence of the acceptor (blank): Specific efflux (%) = Cholesterol efflux (%) – Blank efflux (%).

Statistical analysis

Statistical analyses were performed with the GraphPad prism software version 4.03. Nonlinear regression (sigmoidal dose response) was used to calculate the EC₅₀ values and maximal fold activation. The data are presented as mean ± SD. Statistical evaluation was performed by 1-way analysis of variance (ANOVA) with the Bonferroni post-test or Student's t-test, whichever was appropriate. Differences between groups with a p-value <0.05 were considered statistically significant.

Molecular docking

Docking studies were conducted using AutoDock Vina 1.1. [30] as implemented in LigandScout 4.4. (LigandScout 4.4., Inte:Ligand GmbH) The protein data bank (PDB) structure 6hl1 [11] describing the endogenous ligand CDCA bound to human FXR was selected for the binding mode calculations. Pose prediction accuracy was assessed in a re-docking experiment with excellent results (RMSD <0.1). Default settings were used.

Supporting Information

Supplementary Fig. 1S and details for all reaction steps and analytical data on the synthesis of leoligin and leoligin analogs are available in the Supporting Information.

Acknowledgements

This project was supported by the Austrian Science Fund (FWF): S10710, S10711, and S10704 (NFN-Drugs from Nature Targeting Inflammation) and by the Vienna Anniversary Foundation for Higher Education (H-268438/2018). We thank Daniel Schachner, Scarlet Hummelbrunner, Alexandra Holzer, Lenka Kovářová, Nadja Kühne, and Ulrike Kirchweiger for their excellent technical assistance. We also thank Inte:Ligand GmbH (Vienna) for an academic license for LigandScout 4.4.

Conflict of Interest

The authors declare that they have no conflict of interest.

References

- [1] WHO. Fact sheet on Obesity; 2016. Available at <https://www.who.int/en/news-room/fact-sheets/detail/obesity-and-overweight>. Accessed December 15, 2019
- [2] Makishima M, Okamoto AY, Repa JJ, Tu H, Learned RM, Luk A, Hull MV, Lustig KD, Mangelsdorf DJ, Shan B. Identification of a nuclear receptor for bile acids. *Science* 1999; 284: 1362–1365
- [3] Chow MD, Lee YH, Guo GL. The role of bile acids in nonalcoholic fatty liver disease and nonalcoholic steatohepatitis. *Mol Aspects Med* 2017; 56: 34–44
- [4] Calkin AC, Tontonoz P. Transcriptional integration of metabolism by the nuclear sterol-activated receptors LXR and FXR. *Nat Rev Mol Cell Biol* 2012; 13: 213–224
- [5] Forman BM, Goode E, Chen J, Oro AE, Bradley DJ, Perlmann T, Noonan DJ, Burka LT, McMorris T, Lamph WW, Evans RM, Weinberger C. Identification of a nuclear receptor that is activated by farnesol metabolites. *Cell* 1995; 81: 687–693
- [6] Renga B, Migliorati M, Mencarelli A, Fiorucci S. Reciprocal regulation of the bile acid-activated receptor FXR and the interferon-gamma-STAT-1 pathway in macrophages. *Biochim Biophys Acta* 2009; 1792: 564–573
- [7] De Magalhaes Filho CD, Downes M, Evans RM. Farnesoid X receptor an emerging target to combat obesity. *Dig Dis* 2017; 35: 185–190
- [8] Massafra V, Pellicciari R, Gioiello A, van Mil SWC. Progress and challenges of selective farnesoid X receptor modulation. *Pharmacol Ther* 2018; 191: 162–177
- [9] Mudaliar S, Henry RR, Sanyal AJ, Morrow L, Marschall HU, Kipnes M, Adorini L, Sciacca CI, Clopton P, Castelloe E, Dillon P, Pruzanski M, Shapiro D. Efficacy and safety of the farnesoid X receptor agonist obeticholic acid in patients with type 2 diabetes and nonalcoholic fatty liver disease. *Gastroenterology* 2013; 145: 574–582.e1
- [10] Neuschwander-Tetri BA, Loomba R, Sanyal AJ, Lavine JE, Van Natta ML, Abdelmalek MF, Chalasani N, Dasarthy S, Diehl AM, Hameed B, Kowdley KV, McCullough A, Terrault N, Clark JM, Tonascia J, Brunt EM, Kleiner DE, Doo E, Network NCR. Farnesoid X nuclear receptor ligand obeticholic acid for non-cirrhotic, non-alcoholic steatohepatitis (FLINT): a multi-centre, randomised, placebo-controlled trial. *Lancet* 2015; 385: 956–965
- [11] Merk D, Sreeramulu S, Kudlinzki D, Saxena K, Linhard V, Gande SL, Hiller F, Lamers C, Nilsson E, Aagaard A, Wissler L, Dekker N, Bamberg K, Schubert-Zsilavecz M, Schwalbe H. Molecular tuning of farnesoid X receptor partial agonism. *Nat Commun* 2019; 10: 2915
- [12] Hiebl V, Ladurner A, Latkolik S, Dirsch VM. Natural products as modulators of the nuclear receptors and metabolic sensors LXR, FXR and RXR. *Biotechnol Adv* 2018; 36: 1657–1698
- [13] Duwensee K, Schwaiger S, Tancevski I, Eller K, van Eck M, Markt P, Linder T, Stanzl U, Ritsch A, Patsch JR, Schuster D, Stuppner H, Bernhard D, Eller P. Leoligin, the major lignan from Edelweiss, activates cholesterol ester transfer protein. *Atherosclerosis* 2011; 219: 109–115
- [14] Scharinger B, Messner B, Turkcan A, Schuster D, Vuorinen A, Pitterl F, Heinz K, Arnhard K, Laufer G, Grimm M, Stuppner H, Oberacher H, Eller P, Ritsch A, Bernhard D. Leoligin, the major lignan from Edelweiss, inhibits 3-hydroxy-3-methyl-glutaryl-CoA reductase and reduces cholesterol levels in ApoE^{-/-} mice. *J Mol Cell Cardiol* 2016; 99: 35–46
- [15] Wang L, Ladurner A, Latkolik S, Schwaiger S, Linder T, Hosek J, Palme V, Schilcher N, Polansky O, Heiss EH, Stangl H, Mihovilovic MD, Stuppner H, Dirsch VM, Atanasov AG. Leoligin, the major lignan from Edelweiss (*Leontopodium nivale* subsp. *alpinum*), promotes cholesterol efflux from THP-1 macrophages. *J Nat Prod* 2016; 79: 1651–1657
- [16] Waltenberger B, Atanasov AG, Heiss EH, Bernhard D, Rollinger JM, Breuss JM, Schuster D, Bauer R, Kopp B, Franz C, Bochkov V, Mihovilovic MD, Dirsch VM, Stuppner H. Drugs from nature targeting inflammation (DNTI): a successful Austrian interdisciplinary network project. *Monatsh Chem* 2016; 147: 479–491
- [17] Atanasov AG, Waltenberger B, Pferschy-Wenzig EM, Linder T, Wawrosch C, Uhrin P, Temml V, Wang L, Schwaiger S, Heiss EH, Rollinger JM, Schuster D, Breuss JM, Bochkov V, Mihovilovic MD, Kopp B, Bauer R, Dirsch VM, Stuppner H. Discovery and resupply of pharmacologically active plant-derived natural products: a review. *Biotechnol Adv* 2015; 33: 1582–1614
- [18] Linder T, Liu R, Atanasov AG, Li Y, Geyrhofer S, Schwaiger S, Stuppner H, Schnurch M, Dirsch VM, Mihovilovic MD. Leoligin-inspired synthetic ligands with selectivity for cell-type and bioactivity relevant for cardiovascular disease. *Chem Sci* 2019; 10: 5815–5820
- [19] Schuster D, Markt P, Grienke U, Mihaly-Bison J, Binder M, Noha SM, Rollinger JM, Stuppner H, Bochkov VN, Wolber G. Pharmacophore-based discovery of FXR agonists. Part I: model development and experimental validation. *Bioorg Med Chem* 2011; 19: 7168–7180
- [20] Li G, Kong B, Zhu Y, Zhan L, Williams JA, Tawfik O, Kassel KM, Luyendyk JP, Wang L, Guo GL. Small heterodimer partner overexpression partially protects against liver tumor development in farnesoid X receptor knock-out mice. *Toxicol Appl Pharmacol* 2013; 272: 299–305
- [21] Baker AD, Malur A, Barna BP, Kavuru MS, Malur AG, Thomassen MJ. PPAR-gamma regulates the expression of cholesterol metabolism genes in alveolar macrophages. *Biochem Biophys Res Commun* 2010; 393: 682–687
- [22] Chawla A, Boisvert WA, Lee CH, Laffitte BA, Barak Y, Joseph SB, Liao D, Nagy L, Edwards PA, Curtiss LK, Evans RM, Tontonoz P. A PPAR gamma-LXR-ABCA1 pathway in macrophages is involved in cholesterol efflux and atherogenesis. *Mol Cell* 2001; 7: 161–171
- [23] Aravindhan K, Webb CL, Jaye M, Ghosh A, Willette RN, DiNardo NJ, Jucker BM. Assessing the effects of LXR agonists on cellular cholesterol handling: a stable isotope tracer study. *J Lipid Res* 2006; 47: 1250–1260
- [24] Costet P, Luo Y, Wang N, Tall AR. Sterol-dependent transactivation of the ABC1 promoter by the liver X receptor/retinoid X receptor. *J Biol Chem* 2000; 275: 28240–28245
- [25] Repa JJ, Turley SD, Lobaccaro JA, Medina J, Li L, Lustig K, Shan B, Heyman RA, Dietschy JM, Mangelsdorf DJ. Regulation of absorption and ABC1-mediated efflux of cholesterol by RXR heterodimers. *Science* 2000; 289: 1524–1529
- [26] Schwartz K, Lawn RM, Wade DP. ABC1 gene expression and ApoA-I-mediated cholesterol efflux are regulated by LXR. *Biochem Biophys Res Commun* 2000; 274: 794–802
- [27] Mandal PK, Maiti G, Roy SC. Stereoselective synthesis of polysubstituted tetrahydrofurans by radical cyclization of epoxides using a transition-metal radical source. application to the total synthesis of (±)-methylenolactonin and (±)-protolichesterinic acid. *J Org Chem* 1998; 63: 2829–2834
- [28] RajanBabu TV, Nugent WA. Selective generation of free radicals from epoxides using a transition-metal radical. a powerful new tool for organic synthesis. *J Am Chem Soc* 1994; 116: 986–997
- [29] Wang L, Palme V, Rotter S, Schilcher N, Cukaj M, Wang D, Ladurner A, Heiss EH, Stangl H, Dirsch VM, Atanasov AG. Piperine inhibits ABCA1 degradation and promotes cholesterol efflux from THP-1-derived macrophages. *Mol Nutr Food Res* 2017; 61: 1500960
- [30] Trott O, Olson AJ. AutoDock Vina: improving the speed and accuracy of docking with a new scoring function, efficient optimization, and multi-threading. *J Comput Chem* 2010; 31: 455–461
- [31] Flatt B, Martin R, Wang TL, Mahaney P, Murphy B, Gu XH, Foster P, Li J, Pircher P, Petrowski M, Schulman I, Westin S, Wrobel J, Yan G, Bischoff E, Daige C, Mohan R. Discovery of XL335 (WAY-362450), a highly potent, selective, and orally active agonist of the farnesoid X receptor (FXR). *J Med Chem* 2009; 52: 904–907